

## AVOIDING FRACTURE INSTABILITY IN WEDGE SPLITTING TESTS BY MEANS OF NUMERICAL SIMULATIONS

J. LIAUDAT\*, D. GAROLERA\*, A. MARTÍNEZ\*, I. CAROL\*,  
M.R. LAKSHMIKANTHA<sup>†</sup> AND J. ALVARELLOS<sup>†</sup>

\* ETSECCPB (School of Civil Engineering-Barcelona)  
UPC (Technical University of Catalonia)  
E-08034 Barcelona

e-mail: joaquin.liaudat@upc.edu, daniel.garolera@upc.edu, ariadna.martinez.e@upc.edu,  
ignacio.carol@upc.edu

<sup>†</sup>CTR-Repsol, 28935 Móstoles (Madrid)  
e-mail: m.lakshmikantha@repsol.com, jose.alvarells@repsol.com

**Key words:** Rock, WST, Fracture Mechanics, FEM, Interface Elements

**Abstract.** In this paper, unstable fracture propagation obtained in a in-house performed experimental Wedge Splitting Test (WST) is simulated by means of the FEM and fracture-based zero-thickness interface elements. In order to obtain a specimen geometry suitable for a stable WST without modifying the remaining significant parameters of the test (machine stiffness and control parameter), additional simulations were performed varying the length of the specimen notch, until a load-COD (Crack Opening Displacement) curve without snap-back was obtained. Finally, a new experimental WST with the modified geometry was carried out leading to a stable load-COD curve. In the simulations, elastic continuum elements were used to represent the rock, the steel loading plates and the testing machine compliance via an “equivalent spring”, whereas interface elements were used for the notch and along the potential crack path. The interface elements representing the notch were equipped with linear elastic constitutive law, with very low elastic stiffness  $K_n$  and  $K_t$  so that they do not oppose any significant resistance to opening. For the interface elements along the fracture path, an elastoplastic constitutive model with fracture energy-based evolution laws was used.

### 1 INTRODUCTION

The Wedge Splitting Test (WST) is a method to generate fracture propagation in quasi-brittle materials in order to determine fracture mechanics parameters in mode I, such as the fracture toughness ( $K_{IC}$ ) for the linear theory, or the specific fracture energy ( $G_f^I$ ) for the linear or also non-linear theory [1, 2]. In any case, it is essential that the propagation of the fracture occurs in a stable manner. A WST is stable if no sudden

drop of the the applied load follows the peak. that is, a stable WST shows an overall load-COD (Crack Opening Displacement) diagram with a descending branch after peak load is reached [1]. The stability of the fracture propagation depends on the interaction between of the control parameter chosen (displacement of the testing machine actuator or COD), the stiffness of the testing machine, the specimen stiffness and geometry, as well as the material properties.

In this paper, experimental results from an unstable WST are simulated via a Finite Element model in order to interpret the reasons of the unstable propagation of the fracture, and to explore possible solutions for avoiding it in following tests. Afterwards, based on the conclusions reached in the first analysis, a new WST test was performed in which the specimen geometry was slightly modified. As result, stable WST was obtained, proving the effectiveness of the proposed procedure.

## 2 WST EXPERIMENTAL SET-UP

### 2.1 Principles

The method uses cylindrical or prismatic specimens in which a notch has been cut in order to prefigure the cracking path. A pair of steel loading plates equipped with roller bearings is glued to both sides of the notch mouth, and lateral opening displacement of the rollers is imposed through a wedge moving vertically down in order to create a crack. A scheme of the test setup and a free body diagram of forces on the wedge are shown in Fig. 1, taken from Ref. [3]. The horizontal force applied to the specimen ( $P_H$ ) is calculated by means of Eq. (1), where  $P_V$  is the vertical load applied,  $\theta$  is the wedge angle and  $\mu$  is the coefficient of friction between wedge and roller.

$$P_H = \frac{1 - \mu \tan \theta}{2(\mu + \tan \theta)} P_V \quad (1)$$

If the fracture process is stable, the specific fracture energy of the material  $G_f^I$  can be obtained from the  $P_H - COD$  response of the specimen using Eq. (2), where  $A_l$  is the surface of the ligament area ( $A_l = L \cdot D$ , in Fig. 2).

$$G_f^I = \frac{1}{A_l} \int_0^{+\infty} P_H dCOD \quad (2)$$

The displacement of the wedge is imposed by means of a testing machine with a closed-loop control, which can be controlled in two different ways: (1) by fixing the vertical displacement rate of the machine actuator, or (2) by fixing a COD rate. According with Brühwiler and Wittmann [1], the stability of the fracture process in each case depends on fulfilling the following generic conditions:

$$\text{Actuator control : } l_{ch} > K \cdot L_c \cdot (k_s/k_M + 1) \quad (3)$$

$$\text{COD control : } l_{ch} > K \cdot L_c \quad (4)$$

where  $l_{ch}(= E \cdot G_f^I / f_t^2)$  is the characteristic length of the material ( $E$  is the elastic modulus,  $f_t$  is the tensile strength),  $K$  is a constant depending on the specimen geometry,  $L_c$  is the

cantilever length,  $k_s$  is the specimen stiffness, and  $k_M$  is the testing machine (including the WST device) stiffness.

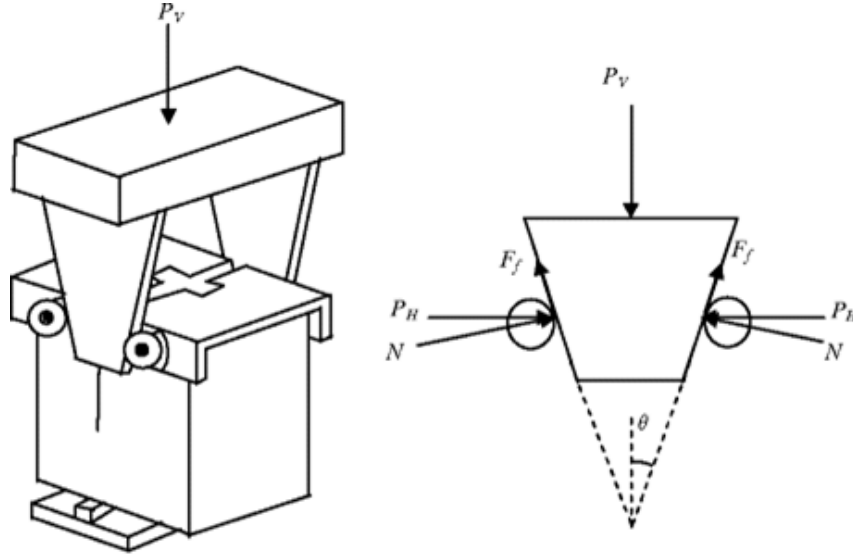


**Figure 1:** Details of the Wedge Splitting Test (WST) set up: test setup of the WST specimen (left), and free body diagram of forces (right). Taken from Ref. [3].

In this paper, results of two experimental WST performed on core samples from the same source are presented. In both cases, the WST were performed controlling the actuator displacement. In the first test, an unstable fracture was obtained. In order to avoid this in the following test, the specimen stiffness  $k_s$  was reduced according to the procedure described in Sec. 4.

## 2.2 Apparatus

A WST device similar to the one illustrated in Fig. 1 was placed in a “ELE Digital Tritest 100 testing machine” (loading capacity 500 kN). As mentioned above, the test were performed controlling displacement rate of the actuator. The vertical load was measured using a load cell UtilCell 610 (nominal load 25 kN, linearity error  $< \pm 0.25\%$  F.S.) with signal conditioning amplifiers Krenel CEL/M010. The COD was measured with two LVDT sensors RDP GT2500 ( $\pm 2.5$  mm, linearity error  $< \pm 0.1\%$  F.S.), with signal conditioning amplifiers RDP S7AC. The LVDTs were placed in the axis of the horizontal splitting force, one on each side of the specimen (COD1 on side 1, COD2 on side 2). The experimental COD informed in Sec. 4 is the average of these two measurements. Finally, the data from the sensors was acquire through a ELE Automatic Data Acquisition unit.

## 2.3 Specimens

The experimental WSTs were performed on a calcareous rock from a deep perforation core of 100 mm diameter. No physical properties of this rock were known at the moment of performing the WST. In order to prepare the specimens for the WSTs, two consecutive

sections of 100 mm length were cut from the perforation core. Then, a groove and a notch were cut in each specimen according to the geometry and dimensions indicated in Fig. 2, where  $L$  is the ligament length and  $D$  the ligament depth. In order to force a straight crack propagation path, a 5 mm-deep groove was cut on both sides of the specimen, on the circular surfaces perpendicular to its axis (see perspective view in Fig. 2).

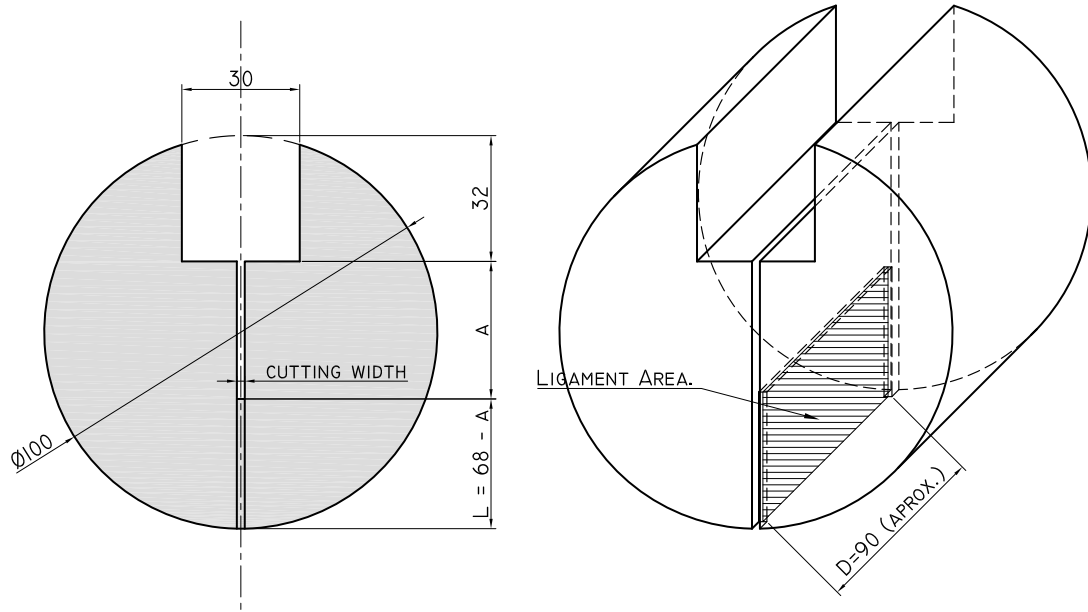


**Figure 2:** Dimensions of the WST specimen. Taken from Ref. [5].

The ligament length is given generically as  $L$  in Fig. 2 since it is the geometry parameter to be determined in Sec. 4 in order to avoid fracture instability. Note that by reducing  $L$  one can reduce the specimen stiffness ( $k_s$ ) and, eventually, make stable an originally unstable test configuration by fulfilling the relationship stated in Eq. (3). On the other hand, the ligament area must be large enough to be representative of the macroscopic material behavior.

### 3 NUMERICAL MODELLING OF THE WST

The model geometry and the FE mesh used are presented in Fig. 3, where grey elements represent the rock, blue elements represent the steel loading plates and magenta elements represent an “equivalent spring” on behalf of the machine compliance. The notch (green line) and the fracture path (red line) on the rock were represented by zero-thickness interface elements.

The lower roller support was simulated by restricting the vertical displacement of the lowest nodes. The horizontal displacements imposed on the roller bearings by the testing machine were simulated by imposing horizontal displacements of same values and opposite sign, on the equivalent springs.

For continuum elements (rock, plates and equivalent spring), isotropic linear elastic materials were assumed. The interface elements representing the notch were equipped with a linear elastic constitutive law and very low elastic stiffness  $K_n$  and  $K_t$ , so that they do not oppose any significant resistance to opening. The constitutive model used for the interface elements along the fracture path was the elastoplastic constitutive model with fracture energy-based evolution laws described in detail in Ref. [4].

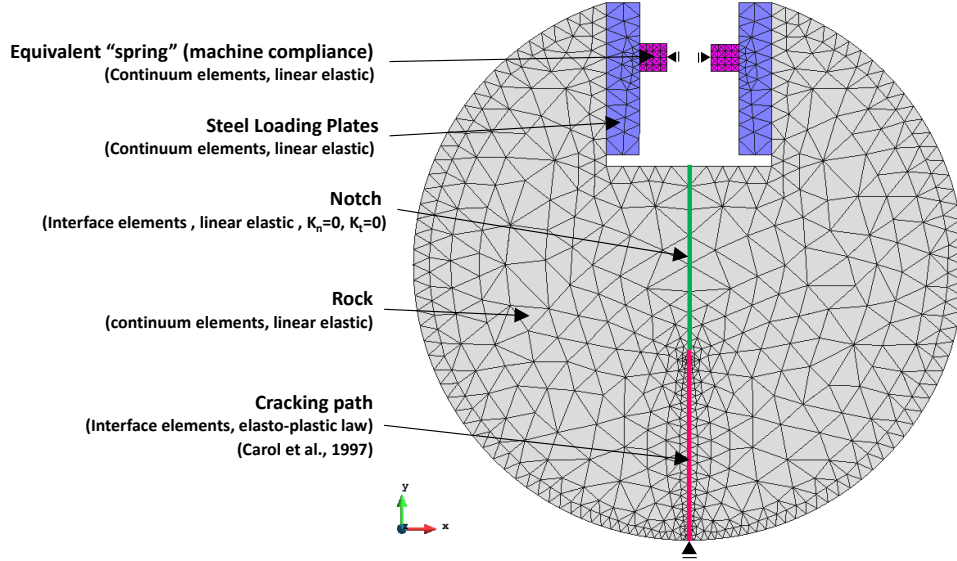


Figure 3: FE mesh and boundary conditions.

The stiffness of the  $5 \times 5$  mm equivalent spring has been calibrated in a previous work [5], resulting in an elastic modulus  $E = 700$  MPa with a Poisson's coefficient of  $\nu = 0$ . For the steel loading plates, conventional values of  $E = 200$  GPa and  $\nu = 0.30$  were adopted.

No mechanical properties of the rock were known at the moment of performing the WST and no additional tests, such as compression tests, were performed. Therefore, the mechanical parameters used in the simulations had to be obtained by fitting the experimental WST curves presented in the next Section.

## 4 NUMERICAL AND EXPERIMENTAL RESULTS

### 4.1 Specimen 1 - Unstable fracture

The  $P_H - COD$  curve obtained from the first tested specimen (Specimen 1) is plotted in gray in Fig. 4. This specimen, with a ligament length of  $L = 34.5$  mm and a ligament depth of  $D = 90$  mm, developed an unstable fracture propagation as it can be inferred from the abrupt load drop in the  $P_H - COD$  curve after peak. This behavior suggests that the stiffness relation between the testing machine and the specimen was not high enough to guarantee a stable fracture process. For the following specimen, not being possible to increase the stiffness of the machine, it was decided to reduce the stiffness of the specimen by reducing the length of the ligament ( $L$ ).

In order to illustrate the beneficial effect of reducing  $L$  on the fracture stability, Fig. 4 shows some  $P_H - COD$  of curves obtained from the simulations performed with tentative mechanical parameters of the rock for different  $L$  values, together with the experimental results. The red curve, corresponding to a ligament length equal to the one of Specimen 1, exhibits a snapback behavior, which explains the unstable load drop of the experimental curve. As the ligament length is reduced, the snapback is reduced until it completely disappears. The results suggested that a ligament length of about 20 mm would assure a stable fracture process.

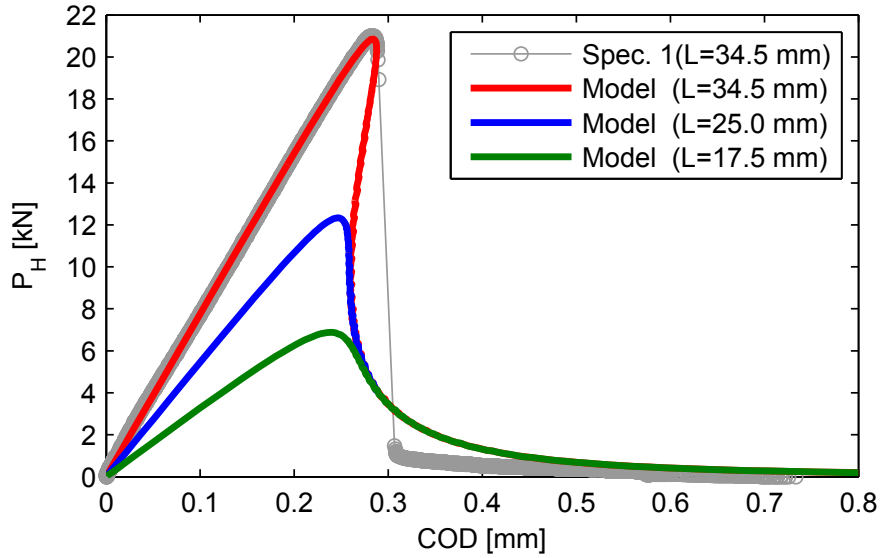


**Figure 4:**  $P_H - COD$  curve from experimental WST of Specimen 1 and from model simulations performed with different ligament lengths  $L$ . All the curves are normalized to a specimen depth of 1000 mm.

#### 4.2 Specimen 2 - Stable fracture

Specimen 2 was tested with a ligament length of 19.5 mm. As predicted, the  $P_H - COD$  curve obtained (Fig. 5) indicates a stable fracture process. The specific fracture energy ( $G_f^I$ ) measured was 52.9 N/m.

Finally, the experimental WST on Specimen 2 was numerically simulated using the measured value of  $G_f^I$ . The tensile strength ( $f_t$ ) and the elastic modulus of the rock ( $E$ ) were adjusted by trial and error to 10 MPa and 45 GPa, respectively, in order to fit the experimental  $P_H - COD$  curve, as it is shown in Fig. 5.

### 5 CONCLUDING REMARKS

- Numerical modelling of experimental WST has helped to interpret failed results and to solve the underlying problems. Additionally, it has allowed to indirectly estimate other mechanical parameters of the rock ( $E$ ,  $f_t$ ) besides the specific fracture energy.

- More WST are needed in order to assess the statistical reliability of the measured  $G_f^I$  value reported.
- Standard uniaxial and triaxial tests would be also desirable in order to verify the values estimated from retrofitting of numerical simulations.

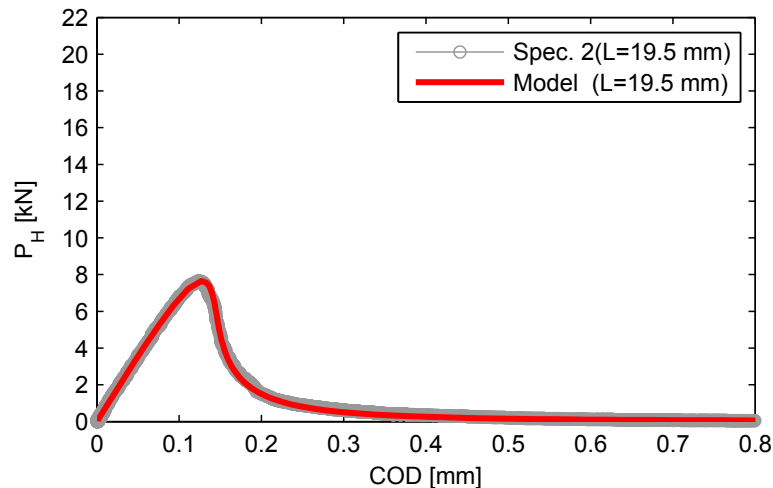


**Figure 5:**  $P_H$ – $COD$  curves from rock specimens obtained experimentally and from numerical simulation. Results are normalized to a specimen depth of 1000 mm.

## ACKNOWLEDGEMENT

This work was partially supported by research grant BIA2016-76543-R from MEC (Madrid), which includes European FEDER funds and by AGAUR / Generalitat de Catalunya (Barcelona) through project 2014SGR-1523. The support from REPSOL for this research is also gratefully acknowledged. The third author also acknowledges AGAUR for her FI doctoral fellowship.

## REFERENCES

- [1] Brühwiler, E. and Wittmann, F. The wedge splitting test, a new method of performing stable fracture mechanics tests. *Engineering Fracture Mechanics* (1990) **35**(1):117–125.
- [2] Saouma, V., Broz, J., Brühwiler, E. and Boggs, H. Effect of aggregate and specimen size on fracture properties of dam concrete. *J. Mater. Civ. Eng.* (1991)(3):204–218.
- [3] Kumar, S. and Barai, S.V., *Concrete fracture models and applications*. Springer Science & Business Media (2011).
- [4] Carol, I., Prat, P. and López, C.M., Normal/Shear Cracking Model: Application to Discrete Crack Analysis. *Journal of Engineering Mechanics* (1997) **123**(8):765–773.

- [5] Liaudat, J., Garolera, D., Martínez, A., Carol, I., Lakshmikantha, M.R. and Alvarells, J. Numerical modelling of the Wedge Splitting Test in rock specimens, using fracture-based zero-thickness interface elements. In: Oñate E., Owen D.R.J., Peric D., Chiumeti M. (eds), *XIII International Conference on Computational Plasticity - Fundamentals and Applications*. CIMNE, Barcelona (2015), pp 974-981.